

Optimal decomposition of travel times measured by probe vehicles using a statistical traffic flow model

A. Hofleitner *student member, IEEE* and A. Bayen, *member, IEEE*

Abstract—Sparse location measurements of probe vehicles are a promising data source for arterial traffic monitoring. One common challenge in processing this source of data is that vehicles are sampled infrequently (on the order of once per minute), which means that many vehicles will travel several links of the network between consecutive measurements. In this article, we propose an optimal decomposition of path travel times of probe vehicles to link travel times for each link traversed. From a model of arterial traffic dynamics, we derive probability distributions of travel times. We prove that these distributions are mixtures of log-concave distributions and derive convex formulations of the travel time allocation problem. We validate our approach using detailed video camera data from the Next Generation Simulation project (NGSIM).

I. INTRODUCTION

Traffic congestion is an important negative externality for modern society [21]. An essential step towards active congestion control is the development of ubiquitous traffic monitoring and operations systems. Historically, these systems have been mostly limited to highways and have relied on data feeds from dedicated sensing infrastructure (loop detectors, radars, video cameras, etc.). For arterials, probe vehicle data, such as fleet data, participatory sensing data or RFID tag data, is the only significant data source with the prospect of global coverage in the future. Common sampling strategies provide sparse information on the location of a vehicle on its trajectory, *e.g.* location reported periodically in time (or in space) on the average of once per minute (once every few hundred meters). Probe vehicle data comes with unprecedented challenges to infer traffic conditions. Map matching [22] and path reconstruction [14], [4] algorithms map the noisy measurements to the road network and infer the trajectory between successive location measurements. Filtering algorithms leverage information on the dynamics of traffic [6] to detect outliers and remove specific behaviors of the probe vehicles sending their location. For example, one

can remove trajectories representing a taxi making a U-turn to pick-up a passenger or a taxi loading or unloading passengers (using a flag signaling if the taxi is hired [1]). Finally, specific algorithms must be developed to use this novel data for traffic estimation and prediction.

Numerous algorithms rely on high frequency probe data [22], fixed sampling locations [11], link travel time measurements [10], [17], [3] or link congestion levels [8] to infer (and predict) the traffic conditions on the road network. These algorithms require that travel times of individual links be computed from the path travel times of the probe vehicles. This computation is called *travel time allocation* or *travel time decomposition* [9] and is the main focus of this article. This problem has been receiving increasing attention as researchers and public entities realize the importance of sparsely sampled probe vehicles for the development of ubiquitous traffic monitoring and operations systems. The formalization of the intuitive idea that vehicles are more likely to experience delays close to intersections [9] shows significant improvements compared to an allocation proportional to the free flow travel time. The modeling of vehicle dynamics on an arterial network is promising to accurately solve the travel time allocation problem and is recommended by traffic data collection guidelines [26]. Virtual floating car data and simulation [24] are another method, provided that loop detector measurements and precise signal timing information are available, which limits the applicability on large arterial networks. Algorithms specific to highway traffic also address travel time decomposition problems [18] but their generalization to arterial traffic is challenging.

In this article, we assume minimal a priori information, mainly the geographical road network and the locations of signals. In particular, we do not assume the availability of signal timing, free flow speed or flows. Local authorities and traffic management centers keep a (mostly paper based) nomenclature of signal timings and obtaining detailed information on signal timings on large networks is a long and difficult process. In Section II, we use well-established traffic flow modeling approaches relying on hydrodynamic theory [15], [20], [7] for periodic flows. We develop a statistical model of arterial traffic

Ph.D. student, Electrical Engineering and Computer Science, UC Berkeley, CA and UPE/IFSTTAR/GRETTIA, France (e-mail: aude.hofleitner@polytechnique.edu). Corresponding author

Professor, Electrical Engineering and Computer Sciences, Civil and Environmental Engineering, UC Berkeley

dynamics and derive *probability distribution functions* (pdf) of travel times between arbitrary locations [12], which we prove to be finite mixtures of log-concave distributions. We formulate the optimal travel time allocation problem as a log-likelihood maximization problem in Section III. Because the distributions are mixtures of log-concave distributions, the travel time allocation problem is not convex and we use the structure of the finite mixture model to formulate the optimal travel time allocation as the solution of a *convex optimization problem*. The number of stops on a path is not limited a priori (which is one of the limitations of the formulation of the problem solved in [9]). We assess the accuracy of the travel time allocation algorithm in Section IV using the *Next Generation Simulation* (NGSIM) arterial traffic data [2] to simulate probe vehicles sending their location with varying frequencies and compare our travel time allocation to the actual travel times of the vehicles on each link.

Note that the travel time allocation problem is often ill-posed. To illustrate this fact, consider a vehicle traversing two successive links and sending its location at the beginning of the first link and the end of the second link. Assume that both links have similar traffic conditions and that the vehicle stops once at a signal. Without additional information, we cannot confidently determine which link the vehicle stopped on and thus solve the travel time allocation problem. This issue arises in all travel time allocation algorithms considering this specific problem and we do not claim to solve it in this article. Our approach chooses the most likely travel time allocation and in particular the most likely delays (both in terms of location and duration) experienced by each probe vehicle.

II. TRAVEL TIME DISTRIBUTIONS DERIVED FROM A HYDRODYNAMIC THEORY FOR PERIODIC FLOWS

In this section, we present specific assumptions common in the traffic engineering community to model arterial traffic dynamics. We analyze the probability of delay of the vehicles traveling on the network and derive the pdf of travel times between arbitrary locations on each link of the network (See [12] for the details of the derivations).

A. Assumptions

Arterial traffic is modeled as a dynamic stochastic process, parameterized by the characteristics of the road network, the signal timing and the driving behavior of the vehicles. We do not assume prior information on the parameters of the model, which can be learned empirically using historical data.

1. *Hydrodynamic fluid assumption*: we model vehicular flow as a continuum and represent it with macroscopic variables of *flow* $q(x, t)$ (veh/s), *density* $\rho(x, t)$ (veh/m) and *velocity* $v(x, t)$ (m/s). The definition of flow gives the following relation between these three variables [15], [20]: $q(x, t) = \rho(x, t)v(x, t)$. We make the assumption of a triangular fundamental diagram parameterized by v_f , the free flow speed (m/s), ρ_{\max} , the jam (or maximum) density (veh/m) and q_{\max} , the capacity (veh/m). For a given road segment of interest, the vehicles arrive into the link with a spatial spacing called arrival density ρ_a . We do not take into account lane changes, passing or merging in this model. For an arterial link with several lanes, we assume that there is one queue per lane, with its own dynamics. The parameters of the road network and the level of congestion may be different on each lane (*e.g.* to model turning movements) or equal (to limit the number of parameters of the model). In this article, we consider that all lanes have the same queue length and do not model the different phases of traffic signals due to dedicated turns.

2. *Stationarity of traffic*: there exist time intervals (on the order of five to fifteen minutes) during which the parameters of the light cycles (red time R and cycle time C) and the arrival density ρ_a are constant. In fact, for numerous signals, the cycle parameters are constant throughout the day or for long time intervals (*e.g.* night, morning rush hour, day, evening rush hour). We assume that there is no consistent increase or decrease in the length of the queue, nor instability over time. With these assumptions, the traffic dynamics are periodic with period C . Note that the assumption of constant ρ_a amounts to neglecting the effects of light synchronization on the arrival rate. This strong assumption enables to keep the derivations of the model analytical and we will discuss how it can be relaxed in Remark 1. The assumption of stationarity is justified if we are interested in studying trends in traffic conditions, rather than fluctuations. The duration of time intervals during which traffic is assumed stationary may depend on the time of the day as conditions may change more rapidly at the beginning and at the end of rush hour periods. We define two discrete traffic regimes: *undersaturated* and *congested*, depending on the presence or the absence of a remaining queue when the light switches from green to red. In the undersaturated regime, the queue is called the *triangular queue* and has length l_{\max} . In the congested regime, there is a *remaining queue*, with length l_r . The congested regime is a short time approximation of a saturation level equal to one (as many vehicles enter and exit during a cycle) with a pre-existing queue l_r .

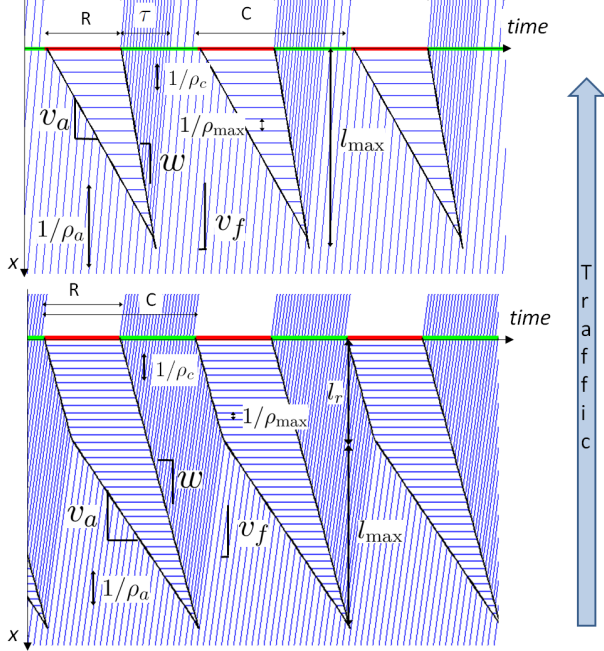


Fig. 1. Space-time diagram of trajectories representing the assumptions of arterial traffic dynamics. **(Top)** Undersaturated regime. **(Bottom)** Congested regime.

Over time, the length of the queue is piecewise constant with possible discontinuities in between time intervals. We illustrate these dynamics in Figure 1.

3. *Model for differences in driving behavior*: the free flow pace p_f (inverse of the free flow speed) is not the same for all vehicles: it is modeled as a *random variable* (r.v.) with vector of parameter θ_p . In the following, we assume that the pdf of free flow pace is *log-concave* (the log of the pdf is concave), which is the case of most common distributions—e.g. the free flow pace has a Gaussian or a Gamma distribution with parameter vector $\theta_p = (\bar{p}_f, \sigma_p)^T$ where \bar{p}_f and σ_p are respectively the mean and the standard deviation of the pace.

B. Probability of delay

Under these simplifying assumptions, we propose an analytical characterization of delay distributions which follows hydrodynamic theory. Previous research on the characterization of delay distribution uses vertical queueing theory to study the probability distribution of delays and queue lengths under stationary assumptions [23], [16]. Vertical queueing theory does not model how vehicles physically queue over the length of the roadway and considers that they stack up upon one another at the stop line of a traffic signal, incurring no delay traveling to the point of congestion, which does not follow the hydrodynamic theory.

We denote by δ_{x_1, x_2} the r.v. representing the delay, due to the presence of traffic signals and the formation

of queues, between locations x_1 and x_2 on an arterial link. The locations x_i also represent the distance to the downstream intersection. The details of the derivation of the pdf of δ_{x_1, x_2} are fully documented and represent a significant amount of technical work available for the reader's convenience in [12]. We summarize the derivations in the case of an undersaturated link and the main results for congested links.

Delays on an undersaturated link: We call η_{x_1, x_2}^u , the fraction of the vehicles entering the link during a cycle that experiences a delay between x_1 and x_2 . The proportion η_{x_1, x_2}^u is computed as the ratio of vehicles joining the queue between x_1 and x_2 , $(\min(l_{\max}, x_1) - \min(l_{\max}, x_2)) \rho_{\max}$, over the total number of vehicles entering the link in one cycle, $v_f C \rho_a$. The proportion of vehicles delayed between x_1 and x_2 is thus:

$$\eta_{x_1, x_2}^u = (\min(x_1, l_{\max}) - \min(x_2, l_{\max})) \frac{\rho_{\max}}{v_f C \rho_a}.$$

The delay experienced when stopping at x is denoted by $\delta^u(x)$ for the undersaturated regime. Because the arrival of vehicles is homogenous, the delay $\delta^u(x)$ increases linearly with x . At the intersection ($x = 0$), the delay is maximal and equals the duration of the red light R . At the end of the queue ($x = l_{\max}$) and upstream of the queue ($x \geq l_{\max}$), the delay is null and we have $\delta^u(x) = R \left(1 - \frac{\min(x, l_{\max})}{l_{\max}}\right)$. Given that the arrival of vehicles is uniform in time, the distribution of the location where the vehicles reach the queue between x_1 and x_2 is uniform in space and the probability to experience a delay between locations x_1 and x_2 is uniform, with support $[\delta^u(x_1), \delta^u(x_2)]$.

Proposition 1 (pdf of delays): The delay experienced on an undersaturated link between locations x_1 and x_2 is a r.v. with finite mixture distribution: a mass probability at 0, with weight $1 - \eta_{x_1, x_2}^u$ and a uniform distribution with support $[\delta^u(x_1), \delta^u(x_2)]$ and weight η_{x_1, x_2}^u . In both the undersaturated and the congested regime, the analytical expression of the pdf of delays depends on the locations x_1 and x_2 and can be expressed as a finite mixture distribution with at most three components. Each component is either a mass or a uniform distribution and corresponds to a different *delay pattern* experienced by the vehicles.

Proof: See [12] for details. The different delay patterns depend on the entrance time of the vehicle with respect to the beginning of a cycle. The delay experienced when stopping at x is piecewise affine in x . Given that the arrivals are uniform in time, the distribution of the location where the vehicles first reach the queue is uniform in space and the probability to experience a delay between two locations is uniform

between a minimum and a maximum delay. The mass distribution is a special case in which the minimum and the maximum delay are equal, corresponding to domains for which the delay experienced when stopping at location x is constant (e.g. non stopping vehicles in the undersaturated regime for which both the minimum and maximum delays are null). ■

Remark 1 (Pdf of delays under platoon arrivals): If the arrival density is piecewise constant with period C (platoons) and its average value is less than or equal to $(1 - R/C)\rho_c$ (saturation less than one), the pdf of delays is a mixture of mass and uniform distributions. The number of components in the mixture depends on the number of platoons and their start and end time with respect to the beginning of the cycle. The proof is a generalization of Proposition 1 and uses the fact that arrivals are uniform within a platoon and that the delay at location x is piecewise affine in x .

C. Finite mixture of log-concave distributions

The travel time y_{x_1, x_2} between x_1 and x_2 is the sum of two independent r.v.: the delay δ_{x_1, x_2} and the free flow travel time $y_{f; x_1, x_2} = p_f(x_1 - x_2)$.

Proposition 2: The pdf of travel times between arbitrary locations on an arterial link is a finite mixture of log-concave distributions with at most three components. Each component corresponds to a different *delay pattern* experienced by the vehicles.

Proof: Since $y_{x_1, x_2} = \delta_{x_1, x_2} + y_{f; x_1, x_2}$ and δ_{x_1, x_2} and $y_{f; x_1, x_2}$ are independent r.v., the pdf of travel times is given by the convolution of the pdf of delays and the pdf of free flow travel times. From the linearity of the convolution and Proposition 1, we know that the travel times have a finite mixture distribution. Each component is the convolution of the pdf of free flow travel times with either a mass or a uniform distribution. Using the fact that log-concavity is closed under multiplication (concavity is closed under addition), and results in the integration of log-concave functions [19], we know that the convolution of two log-concave functions is log-concave [5]. ■

We illustrate the probability distribution of travel times on an undersaturated link in Figure 2. It is a mixture of two log-concave distributions representing the delay patterns “stopping” and “not stopping” on the link. In general, the pdf of travel times g_{x_1, x_2}^i on link i between locations x_1 and x_2 is the sum of $K_i \leq 3$ log-concave components. The k^{th} component, representing the k^{th} delay pattern, has pdf $g_{x_1, x_2}^{i, k}$ and weight $v_k \in [0, 1]$ such that:

$$g_{x_1, x_2}^i = \sum_{k=0}^{K_i} v_k g_{x_1, x_2}^{i, k} \quad \text{and} \quad \sum_{k=0}^{K_i} v_k = 1, \quad v_k \geq 0.$$

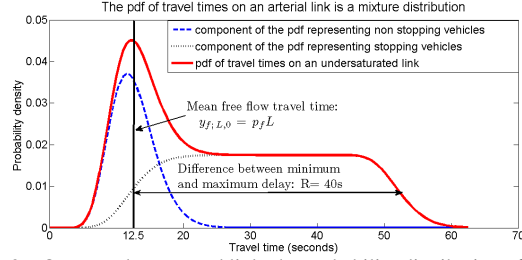


Fig. 2. On an undersaturated link, the probability distribution of travel times (solid line) is a mixture distribution with two components: the vehicles that do not stop on the link and have zero delay (dashed line) and the vehicles that experience delay on the link (dotted line). The illustration is computed for $\eta = 0.7$, $R = 40\text{s}$. The free flow pace is a Gamma r.v. with mean $1/8$ s/m and standard deviation $1/30$ s/m.

The pdf of travel times between arbitrary locations is parameterized by the cycle time C , the red time R , the queue length (l_{\max} in the undersaturated regime and $l_{\max}^s + l_r$ in the congested regime), the saturation queue length l_{\max}^s (length of the triangular queue when the number vehicles that enter and leave the link in a cycle are equal) and the parameters of the free flow pace θ_p .

III. DECOMPOSITION OF THE TRAVEL TIMES TO THE LINKS OF A PATH

A travel time observation from a probe vehicle consists of a travel time over a path defined by multiple (potentially partial) links. We formulate the optimal travel time allocation as the solution of a maximum (log)likelihood problem where the decision variables represent the travel times allocated to each of the (partial) links of the path. We can view the maximum likelihood problem as the estimation of the most likely entrance times (modulo the cycle times) of the vehicle on the links of the path. The objective function is the joint probability of the travel times allocated to each link of the path. However, the analytical derivation of this function from traffic flow theory remains an unresolved problem and we assume that link travel times are independent, which corresponds to discarding the information on the entrance time in a link depending on the entrance time at the previous link.

A. Travel time decomposition

For a vehicle traveling from an origin x_o to a destination x_d through M intersections, we decompose the travel time y_{x_o, x_d} as the sum of travel times on each of the links (Figure 3):

$$y_{x_o, x_d} = \sum_{m=0}^M y_{x_m, x_{m+1}}. \quad (1)$$

For $m \in \{1 \dots M\}$, the point x_m represents the most upstream location on the m^{th} link on the path, $x_0 = x_o$ and $x_{M+1} = x_d$. For $m \in \{0 \dots M\}$, we note i_m the

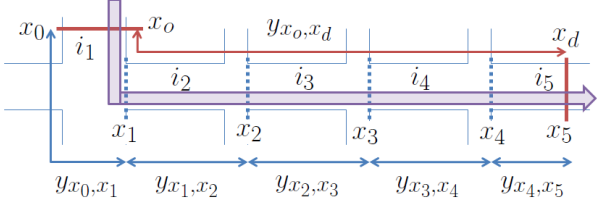


Fig. 3. Travel time allocation: decomposition of the path travel time into (partial) link travel times. Along its trajectory, the vehicle sends location measurements successively at x_o and x_d for a travel time y_{x_o,x_d} . This path extends over five links (numbered i_1 to i_5). The path only spans a fraction of the first and last links (partial links). We decompose the total travel time y_{x_o,x_d} into five (partial) link travel time $(y_{x_m,x_{m+1}})_{m=0\dots4}$ which sum to the total travel time y_{x_o,x_d} .

m^{th} link of the path between x_m and x_{m+1} and we denote by g^{i_m} the pdf of travel times on (partial) link i_m , between x_m and x_{m+1} (Note that we dropped the index x_m, x_{m+1} for notational simplicity).

The optimal decomposition of a travel time y_{x_o,x_d} is the minimizer of the following optimization problem:

$$\underset{(y_{x_m,x_{m+1}})_{m=0}^M}{\text{minimize}} \sum_{m=0}^M -\ln(g^{i_m}(y_{x_m,x_{m+1}})), \text{ s.t. (1). (2)}$$

As formulated above, optimization problem (2) is not convex and we use Proposition 2 to formulate the travel time allocation as a convex optimization program. We propose different algorithms and analyze their performance and accuracy in Section IV.

B. Optimization algorithms

In general, problem (2) is not convex thus first and second order optimization algorithms are only guaranteed to find local optima. Global optimization algorithms [13], [25] can solve the problem of local optima but are out of the scope of this article. We consider a gradient descent algorithm with random starts denoted **Gradient algorithm** and investigate how to exploit the structure of the optimization problem given by Proposition 2 to find convex formulations of (2):

1. **Expectation-Maximization (EM) algorithm:** After an initial allocation $(y_{x_m,x_{m+1}}^0)$ of the travel times to the links of the path (e.g. random allocation, allocation proportional to the mean or the free flow travel times), the algorithm iterates between an analytical computation (E step) and a small scale optimization problem (M step). It is only guaranteed to converge to local optima but exploits the structure of the optimization problem:

E step: at iteration n , the travel time allocated to link i_m is $y_{x_m,x_{m+1}}^n$. Compute the probability $\tilde{\beta}_{i_m,k}^n$ that the vehicle experienced delay pattern k on link i_m :

$$\tilde{\beta}_{i_m,k}^n = \frac{v_k g_{i_m,k} \left(y_{x_m,x_{m+1}}^n \right)}{\sum_{k'=0}^{K_{i_m}} v_{k'} g_{i_m,k'} \left(y_{x_m,x_{m+1}}^n \right)}. \quad (3)$$

M step: solve the convex optimization program (4) and go to E Step until convergence.

$$\underset{(y_{x_m,x_{m+1}}^n)_{m=0}^M}{\text{minimize}} \sum_{m=0}^M \sum_{k=0}^{K_{i_m}} -\tilde{\beta}_{i_m,k} \ln(g^{i_m,k}(y_{x_m,x_{m+1}}^{n+1})), \text{ s.t. (1). (4)}$$

2. **Convex Program or Mixed Integer Convex Program:** Given the model of Section II, a vehicle has one delay pattern on each link of its path. Let $\beta^{i_m,k} \in \{0, 1\}$ be equal to 1 if the vehicle has delay pattern k on link i_m and to 0 otherwise. If the sampling strategy detects the location of stops, the variables $\beta^{i_m,k}$ are known and the travel time allocation amounts to solving the convex optimization problem (4) with $\tilde{\beta}_{i_m,k} = \beta_{i_m,k}$ (**Given stop algorithm**). Sampling strategies rarely provide the value of the binary variables $\beta^{i_m,k}$ which become decision variables in (4), with the constraints

$$\forall m \sum_{k=1}^{K_{i_m}} \beta_{i_m,k} = 1, \quad \forall (m,k) \beta_{i_m,k} \in \{0, 1\}, \quad (5)$$

illustrating that a vehicle has exactly one delay pattern on each link. This problem can be solved by enumerating the $\prod_{m=0}^M K_{i_m}$ convex optimization programs corresponding to the different sets of $(\beta_{i_m,k})_{i_m,k}$ (**Enumeration algorithm**). The complexity is exponential in the number of links traversed by the vehicle but remains tractable (bounds on the number of links and the number of components, $K_{i_m} \leq 3$). We can also solve this problem using a hard EM algorithm (**Hard EM algorithm**), which forces the vehicle to have exactly one delay pattern on each link of the path, instead of using the probability of each delay pattern (3). Given a travel time allocation at iteration n , the hard E step computes $\beta_{i_m,k}^n$ such that it is equal to 1 if delay pattern k is the most likely on link i_m and to 0 otherwise:

$$\beta_{i_m,k}^n = \begin{cases} 1 & \text{if } k = \arg \max_{k' \in K_{i_m}} \tilde{\beta}_{i_m,k'}^n, \\ 0 & \text{otherwise} \end{cases} \quad (6)$$

We recall that $\tilde{\beta}_{i_m,k'}^n$ is computed according to (3). The M step solves (4) with $\tilde{\beta}_{i_m,k} = \beta_{i_m,k}^n$. Similar to the EM algorithm, the hard EM algorithm exploits the underlying structure of the optimization problem but only guarantees convergence to local optima and we use random starts to increase the chances of convergence to the global optimum.

IV. RESULTS

We assess the performance of the model and the algorithms using *Next Generation Simulation* (NGSIM [2]) traffic data on the Peachtree Street network (Atlanta, Georgia). The network consists in twelve 3 lane-links

with five intersections. Automatic processing of video camera data provides detailed trajectories (location every 0.1 seconds) of all the vehicles traveling on the network between 4:00 and 4:15pm on November 8, 2006 (more than 700 trajectories). The traffic conditions are undersaturated, close to saturation. We simulate probe vehicles reporting their location with different sampling frequencies and compute the time spent on each link and the locations of stops between successive measurements to serve as ground truth for the travel time allocation. For each probe measurement, we allocate its travel time according to the optimization algorithms described in Section III and compare the performances to an algorithm which allocates the travel times proportionally to the free flow travel time on each link (**Benchmark algorithm**). Denoting by v_m^f the free flow speed on link m and by $|x_{m+1} - x_m|$ the distance traveled on link m , the travel time allocated to each link m of the path by the benchmark algorithm is given by

$$y_{x_m, x_{m+1}} = \frac{1}{Z} \frac{|x_{m+1} - x_m|}{v_m^f}, \quad (7)$$

where the proportionality constant Z is chosen such that the allocated travel times sum up to the path travel time as stated in (1). We recall the different algorithm presented in this article:

- The *Gradient* algorithm finds local optima of (2) using a gradient descent algorithm
- The *EM* algorithm is an iterative algorithm. At iteration n , it computes $(\tilde{\beta}_{i_m, k}^n)$ for each pair of link m and delay pattern k according to (3) and solves the convex optimization problem (4).
- The *Given stop* algorithm solves the convex optimization problem (4) where the values of $\tilde{\beta}_{i_m, k}$ are equal to $\beta_{i_m, k} \in \{0, 1\}$ and are given by the sampling scheme which detects the location of stops.
- The *Enumeration* algorithm solves a serie of convex optimization problems (4) for each set of $(\beta_{i_m, k})_{m=0}^M$ satisfying (5).
- The *Hard EM* algorithm is an iterative algorithm. At iteration n , it computes $\beta_{i_m, k}^n \in \{0, 1\}$ according to (6) and solves the convex optimization problem (4), with $\tilde{\beta}_{i_m, k} = \beta_{i_m, k}^n$.
- The *Benchmark* algorithm allocates travel times proportionally to the free flow speed on each link (Equation (7)).

A. Convergence and performance analysis

When vehicles remain on the same link between two successive location measurements, the travel time allocation is trivial and is not taken into account in these results. For each probe measurement, we compute

the log-likelihood (objective function of (2)) of the allocations performed by the different algorithms and also report the average computation time (Figure 4, left and center). The algorithms *Given stops*, *Enumeration* and *Hard EM* assume that each vehicle has a specific delay pattern on each link whereas *EM* allows for a mixture of delay patterns and *gradient* does not make any assumption. All the algorithms provide an allocation that is more likely than the *benchmark* and the structure provides better convergence properties (*gradient* has the lowest likelihood of all optimizations). The algorithms *enumeration* and *hard EM* provide similar convergence results but the computation time is much better for *hard EM*. In particular, when the sampling time increases, we see the effect of the exponential computation time on the *enumeration* algorithm. The algorithm *given stop* provides allocations with an average log-likelihood slightly inferior to the *enumeration* and *hard EM* algorithms. Indeed, vehicles may not always experience the most likely delay patterns. However, the small difference in log-likelihoods (in comparison to the benchmark algorithm for example) let us infer that in general, the vehicles experience the most likely delay patterns.

B. Validation of the algorithms

We denote by \hat{y}_q^l the q^{th} travel time allocated on link l and by y_q^l the actual travel time of the probe vehicle (computed from the detailed trajectories). We denote Q_l the number of travel times allocated on link l . We compute the average percentage error on link l as the root mean square error of the allocation and divide by the average travel time TT_l to obtain an average percentage error:

$$e_l = \frac{1}{TT_l} \sqrt{\frac{\sum_{q=1}^{Q_l} (\hat{y}_q^l - y_q^l)^2}{Q_l}}.$$

To have a more compact validation metric, we average the percentage error of the different links (Figure 4, right).

Confirming the assumptions of the model, *given stop* provides the best results. The information on stops is rarely available in current sampling strategies and the algorithms *enumeration* and *hard EM* provide the highest accuracy, with slightly better results but higher computation cost for *enumeration*. The *gradient* algorithm has the least accuracy of the optimization algorithms which underlines the importance of the structure imposed by the other algorithms. As a tradeoff between accuracy and computation time, the hard EM algorithm seems the best suited to solve the optimization problem. It provides an improvement of 35% to 50% compared to

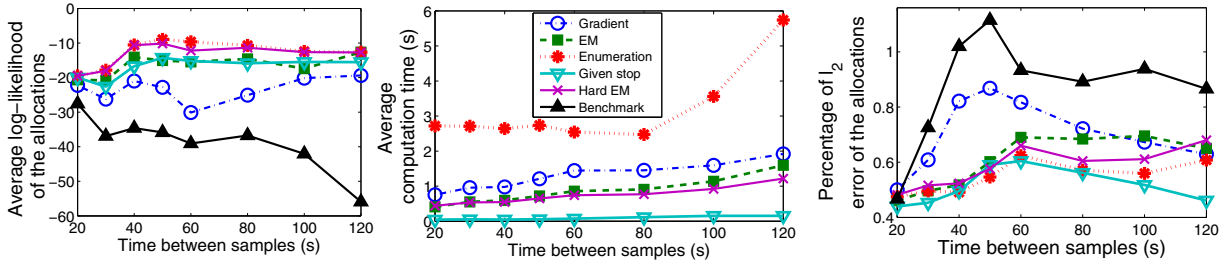


Fig. 4. Performance analysis of the different algorithms as a function of the sampling frequency. (Left) Average log-likelihood of the travel time allocations. (Center) Average computation time. (Right) Average percentage error

the benchmark method for common sampling rates (30 seconds or more between measurements).

V. CONCLUSION

We propose a travel time allocation algorithm based on a comprehensive model of arterial traffic flows that identifies the delay patterns of the vehicles. The travel times are allocated according to the most likely pattern, with an algorithm that exploits the underlying structure of the log-likelihood function. This method provides a significant improvement (up to 50%) compared to a benchmark deterministic method.

REFERENCES

- [1] Cabspotting. <http://www.cabspotting.org>.
- [2] Next Generation Simulation. <http://ngsim-community.org/>.
- [3] S. J. Agbolosu-Amison, B. Park, and I. Yun. Comparative evaluation of heuristic optimization methods in urban arterial network optimization. In *12th Intelligent Transportation Systems Conference (ITSC '09)*, 2009.
- [4] M. Bierlaire and E. Frejinger. Route choice modeling with network-free data. *Transportation Research Part C: Emerging Technologies*, 16(2):187–198, 2008.
- [5] S. P. Boyd and L. Vandenberghe. *Convex optimization*. Cambridge University Press, 2004.
- [6] C. Claudel, M. Nahoum, and A. Bayen. Minimal error certificates for detection of faulty sensors using convex optimization. In *47th Annual Allerton Conference on Communication, Control, and Computing*, Allerton, IL, Sep. 2009.
- [7] C. Daganzo. The cell transmission model: A dynamic representation of highway traffic consistent with the hydrodynamic theory. *Transportation Research B*, 28(4):269–287, 1994.
- [8] C. Furtlehner, J. Lasgouttes, and A. de la Fortelle. A belief propagation approach to traffic prediction using probe vehicles. In *10th Intelligent Transportation Systems Conference (ITSC '07)*, pages 1022–1027, 2007.
- [9] B. Hellinga, P. Izadpanah, H. Takada, and L. Fu. Decomposing travel times measured by probe-based traffic monitoring systems to individual road segments. *Transportation Research Part C*, 16(6):768 – 782, 2008.
- [10] R. Herring, A. Hofleitner, P. Abbeel, and A. Bayen. Estimating arterial traffic conditions using sparse probe data. In *Proceedings of the 13th International IEEE Conference on Intelligent Transportation Systems*, Madeira, Portugal, September 2010.
- [11] R. Herring, A. Hofleitner, S. Amin, T. Abou Nasr, A. Abdel Khalek, P. Abbeel, and A. Bayen. Using mobile phones to forecast arterial traffic through statistical learning. In *Proceedings of the 89th Annual Meeting of the Transportation Research Board*, Washington D.C., 2010.
- [12] A. Hofleitner, R. Herring, and A. Bayen. A hydrodynamic theory based statistical model of arterial traffic. *Technical Report UC Berkeley, UCB-ITS-CWP-2011-2*, http://www.eecs.berkeley.edu/~aude/papers/traffic_distributions.pdf, January 2011.
- [13] R. Horst and H. Tuy. Global optimization: deterministic approaches. *Journal of the Operational Research Society*, 45(5):595–596, 1994.
- [14] T. Hunter, T. Moldovan, M. Zaharia, J. Ma, S. Merzgui, M. Franklin, and A. Bayen. Scaling the mobile millennium system in the cloud. In *submitted to ACM Symposium on Cloud Computing*, 2011.
- [15] M. Lighthill and G. Whitham. On kinematic waves. II. A theory of traffic flow on long crowded roads. *Proceedings of the Royal Society of London. Series A, Mathematical and Physical Sciences*, 229(1178):317–345, May 1955.
- [16] A. J. Miller. Settings for Fixed-Cycle traffic signals. *Operations Research*, 14(4), December 1963.
- [17] X. Min, J. Hu, Q. Chen, T. Zhang, and Y. Zhang. Short-term traffic flow forecasting of urban network based on dynamic STARIMA model. In *Proceedings of the 12th International IEEE Conference on Intelligent Transportation Systems (ITSC '09)*, 2009.
- [18] Q. Ou, J. W. C. Van Lint, and S. P. Hoogendoorn. TravRes: a method for high-resolution traffic speed reconstruction using GPS-based travel-times. In *Proceedings of the 13th International IEEE Conference on Intelligent Transportation Systems (ITSC '10)*, pages 1195–1201, 2010.
- [19] A. Prékopa. On logarithmic concave measures and functions. *Acta Scientiarum Mathematicarum*, 34:335–343, 1973.
- [20] P. Richards. Shock waves on the highway. *Operations Research*, 4(1):42–51, February 1956.
- [21] D. L. Schrank, T. J. Lomax, and Texas Transportation Institute. *2009 Urban mobility report*. Citeseer, 2009.
- [22] A. Thiagarajan, L. Sivalingam, K. LaCurts, S. Toledo, J. Eriksson, S. Madden, and H. Balakrishnan. VTrack: Accurate, Energy-Aware Traffic Delay Estimation Using Mobile Phones. In *7th ACM Conference on Embedded Networked Sensor Systems (SenSys)*, Berkeley, CA, November 2009.
- [23] F. V. Webster. *Traffic signal settings*. Road Research Technical Paper No. 39, Road Research Laboratory, England, published by HMSO, 1958.
- [24] Z. Yang, B. Gong, and C. Lin. Travel time estimate based on floating car. In *2nd International Conference on Intelligent Computation Technology and Automation (ICICTA '09)*, volume 3, pages 868–871, 2009.
- [25] A. Zhigljavsky and A. Zilinskas. *Stochastic global optimization*. Springer, 2007.
- [26] H. J. Zuylen, F. Zheng, and Y. Chen. Using probe vehicle data for traffic state estimation in signalized urban networks. *Traffic Data Collection and its Standardization*, pages 109–127, 2010.